DOE/ER/12126--T2

Nonlinear Optics in Doped Fibers

Final Report

May 1, 1992 - April 30, 1996

Department of Energy
Grant DE-FG03-92ER12126

G. L. Report No. 5456

Principal Investigator

Richard H. Pantell

Edward L. Ginzton Laboratory
Stanford University
Stanford, California 94304-4085

MASTER

DISTRIBUTION OF THIS DOCUMENT IS UNLIMITED

DISCLAIMER

Portions of this document may be illegible in electronic image products. Images are produced from the best available original document.

DOE Final Report

Contract No. DE-FG03-92ER12126

Contract Title: Nonlinear Optics in Doped Fibers

Prepared by:
Michel J. F. Digonnet and Richard H. Pantell
Stanford University, California

September 18, 1996

1. Introduction: Stated Program Objectives

The main objective of this contract was to study a novel scheme to obtain very strong third-order optical nonlinearities in fibers doped with a suitable absorber in order to produce low-power all-optical fiber switches. In these devices, a signal is switched from a first fiber to a second fiber by the application of an optical pump of wavelength different from that of the signal. The pump acts on the nonlinearity of the fiber, resulting from the dopant present in the fiber core, to modify the fiber index. The switch is made of a fiber interferometer which transforms this index modulation into an amplitude modulation. The signal is switched as long as the pump is applied, and it returns to the first fiber when the pump is turned off.

The incentive was to develop switches exhibiting the following properties: (1) low switching power, (2) a short nonlinear fiber (1 cm or shorter) to be able to utilize a short and thus environmentally stable interferometer, (3) fast response time (microsecond or shorter), (4) broad range of signal wavelengths, particularly around 1.55 and 1.32 μm, (5) pump wavelengths readily available from diode lasers, e.g. 800 nm, 980 nm, or 1480 nm, and (6) low signal loss. This research also involved the study of various fiber interferometers to determine the best possible switch architectures, in terms of pump power requirement, stability against environmental temperature fluctuations and possible pump-induced heating of the fiber.

The primary reasons for targeting fibers as a support medium for switches, as opposed to integrated optics where several types of switches have already been

demonstrated, are that (1) an all-fiber device exhibits virtually no internal loss, and (2) it can be readily spliced to a communication fiber to form a lasting connection with negligible loss and excellent thermal and mechanical stability. Such devices did not exist at the beginning of this contract. Prior to this work, the only switches demonstrated in silica fibers utilized the weak Kerr effect of silica. They required very long fibers and/or high peak pump power, which makes them very impractical.

Switches are strongly needed for a large number of important applications. These include periodic self healing communication networks, testing of optical components and fiber links, and re-configurable optical signal processing (which require switching times of the order of ms), asynchronous transmission mode packet switching for local area networks, phased-array radar, and engine performance monitoring (μs switching time), towed sensor arrays and circuit switching (ns to sub-ns), and bit switching and all-optical computing (ps to sub-ps).

The results of the effort expanded under this contract has been published in 23 scientific publications, including 13 scientific journal articles, 9 conference articles, and one thesis. Inventions related to this work are being covered by 4 patents, one issued and three pending. This work has stimulated much interest in the optical community. Several research and R&D groups are now undertaking parallel research of their own on this subject, targeting relatively low speed (μs) low power fiber switches for commercial purposes.

The rest of this report is a summary of the most important tasks carried out, and of the major discoveries made, under this contract. For further reading, a copy of all the aforementioned scientific articles is provided at the end of the report.

2. Summary of Research Activities and Results

2.1 Basic Principle

The switches under study rely on an optical pump of wavelength λ_p to switch a signal of wavelength $\lambda_s \neq \lambda_p$. A typical device configuration is a fiber interferometer, such as the Mach-Zehnder (MZ) shown in Fig. 1. It is configured such that (1) in the absence of pump, all the signal power comes out at the upper output port, and (2) the pump remains in only one of the two MZ arms (the upper arm in Fig. 1). Via the nonlinearity present in the upper arm, the pump induces a change in the index, and thus a change in the phase of the signal, in the upper arm. When the pump power is such that the phase change is π, the signal power is fully switched to the lower output port (see Fig. 1).

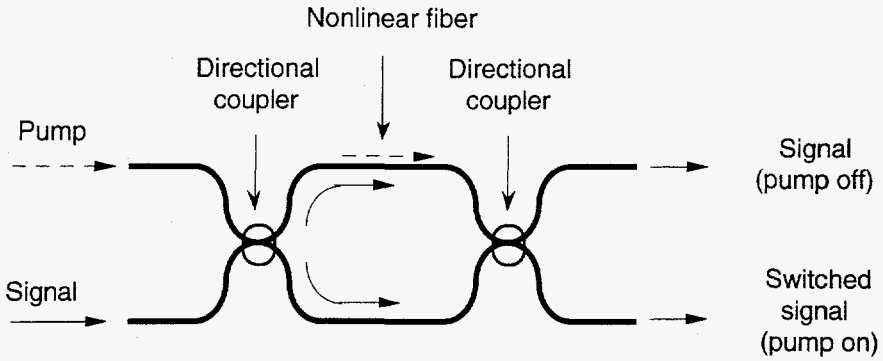

Fig. 1. Schematic of a fiber Mach-Zehnder interferometer used as an optically-pumped nonlinear switch.

The third-order nonlinearity that has been most studied in silica-based fibers for switching is the Kerr effect. It has an extremely fast response time (around a few femtoseconds). It does not introduce absorption loss at either the pump or signal wavelengths, and it operates over the wide transparency range of silica. However, it is notoriously weak, and experimental Kerr fiber switches require a large pump power and/or long fiber for full switching.[1]

The scheme studied here involved considerably stronger resonantly-enhanced third-order nonlinearities, introduced in the fiber by doping its core with a suitable absorber. The dopant is selected such that it exhibits a strong absorption band over a limited region of the spectrum. An optical pump tuned to this band partially depletes the ground state of the dopant, which changes its absorption, and in turn, via the Kramers-Kronig causality principle, its contribution to the core refractive index.

2.2 Model of Switching with a Two-Level Absorber

An advanced theoretical parametric study was developed to model the strength and dynamic behavior of this new type of nonlinearity. This phase of the program was important to predict the pump power and length requirement of a switch, its response time, the residual signal loss, and the signal bandwidth.

The model considers a fiber (or a waveguide) with a core doped with an absorber. The latter is assumed to exhibit a single absorption transition between a ground state (level 1) and an excited state (level 2). (The case of a three-level absorber was also investigated; it differs qualitatively, and only slightly). The transition frequency is centered at ω_{12}, or wavelength λ_{12}. Using the laser rate equations, for a given pump power we calculated the population change induced by the pump, then the change in absorption and finally, by

application of the Kramers-Kronig transformation, the index change induced in the fiber. The latter was then integrated along the fiber length to obtain the pump-induced phase change experienced by a signal of known wavelength. This model relates the phase shift to all the device parameters, i.e. the pump power, fiber length, signal and pump wavelengths, and dopant spectroscopic parameters. It can thus be used to predict, for a given dopant, the parameters of a switch, in particular the switching power, required fiber length, and response time.

2.2.1 Switching Power Requirement

The nonlinear phase shift is proportional to the pump power absorbed by the dopant. This is contrary to the Kerr effect, for which it is proportional to the power traveling in the fiber. The pump power required to produce full switching in a MZ (called switching power and labelled P_{abs}^{π}), is the power needed to produce a π phase shift. It is given by:

$$P_{abs}^{\pi} = \frac{8\pi n^2 hc}{1+\frac{g_2}{g_1}} \frac{\lambda_s}{\lambda_p \lambda_{12}^{\ 3}} \frac{\tau_{rad,2}}{\tau_2} \frac{A}{|g_{12}'(\omega_s)|} \qquad (1)$$

where n is the index of the core, h is Planck's constant, c the speed of light in vacuum, g_1 and g_2 are the degeneracy of level 1 and level 2, respectively, $\tau_{rad,2}$ and τ_2 are the radiative and total lifetime of level 2, respectively, A is the pump mode effective area, and $g_{12}'(\omega_s)$ is the real part of the lineshape function evaluated at the signal angular frequency $\omega_s=2\pi c/\lambda_s$.

The switching power (Eq. 1) scales like the effective pump mode area, as expected for an intensity-dependent process. Since the fiber must carry a single mode at the wavelength of operation ($\lambda_s \approx \lambda_p \approx \lambda_{12}$), the core area A is approximately proportional to λ_{12}^2. Far from resonance, $g_{12}'(\omega_s)$ also scales like λ_{12}. It means that P_{abs}^{π} scales approximately like $1/\lambda_{12}^2$. Everything else being equal, a longer wavelength transition produces a lower switching power. The switching power is also affected by the transition linewidth $\delta\omega_{12}$. At constant signal loss (discussed below), P_{abs}^{π} is proportional to $\delta\omega_{12}^{1/2}$. A narrower linewidth is thus preferable.

2.2.2 Fiber Length Requirement

The power P_{abs}^{π} is independent of fiber length (see Eq. 1). Everything else being equal, this power will induce full switching whether it is absorbed in a short fiber (if the dopant concentration is high) or a long fiber (if the dopant concentration is low). However,

the length affects how much of the *launched* pump power is absorbed, and therefore how much launched power is needed for full switching. For a given dopant concentration, a longer fiber means a larger fraction of the pump is absorbed, i.e. a lower launched pump power is required. If the fiber is too short, it will not absorb sufficient power (i.e. P_{abs}^{π}), even if the launched power is infinite: below a certain minimum length full switching is not possible.

The fiber length required for a switch is determined by the length it takes to absorb the required pump power. Therefore, minimizing the length requires maximizing pump absorption. To this end, the pump wavelength should be centered on the absorption transition ($\lambda_p \approx \lambda_{12}$). The dopant should have a high solubility in silica, and a high oscillator strength transition (for a high absorption cross section). With an oscillator strength even as weak as 10^{-3} and a 0.1 mole% concentration, the required fiber length is in the mm range, which is more than enough for a practical switch: length is not a significant issue.

2.2.3 Range of Signal Wavelengths

To keep the pump power reasonably low, the factor $g_{12}'(\omega_s)$ (see Eq. 1), which depends on the frequency detuning between the signal and the transition, must be relatively large. The factor $g_{12}'(\omega_s)$ decreases as the signal frequency is detuned from the transition frequency,[4,5,22] so in general operating closer to the latter is preferable (although not at the center frequency, since $g_{12}'(\omega_{12})=0$ and the switching power at ω_{12} is thus infinite).

How close to ω_{12} the signal frequency must be depends on the sign of the detuning. When the signal is detuned from the transition center frequency towards shorter wavelengths, i.e. towards the ultraviolet (UV), the factor $g_{12}'(\omega_s)$ decreases to zero, and the switching power becomes infinite (see Eq. 1). Therefore, for signals on the short wavelength side the switch can operate well provided the detuning is not excessive, of the order of a few transition linewidths.

When the signal is detuned towards longer wavelengths, i.e. towards the IR, $g_{12}'(\omega_s)$ decreases to a non-zero asymptotic limit equal to $2/\pi/\omega_{12}$,[21,22] and the switching power remains finite. This limit applies to a Lorentzian, Gaussian, and Voight lineshape. The switch then operates well even for very large detunings. Because this asymptotic value is independent of signal frequency, P_{abs}^{π} is independent of signal wavelength for a signal far enough in the IR (i.e. sufficiently detuned, of the order of $\omega_s/\omega_{12}<0.5$). This is a very important property of resonantly enhanced nonlinearities: any dopant that operates well for a signal near the transition will also operate well in the IR, the frequency range of interest for most applications.

2.2.4 Signal Loss

The absorber is expected to introduce some loss at the signal frequency, which must be kept to a minimum. To do so, the signal wavelength must be detuned sufficiently far from linecenter. However, detuning also increases the switching power, as discussed above. This conflict can be resolved because $g_{12}'(\omega_s)$ decreases much less rapidly with detuning than the imaginary part $g_{12}''(\omega_s)$ of the lineshape function, to which the signal absorption loss is proportional.[4,5,22] For large detunings and a Lorentzian lineshape, $g_{12}'(\omega_s)$ decreases as $(\omega_{12}-\omega_s)^{-1}$, while $g_{12}''(\omega_s)$ decreases as $(\omega_{12}-\omega_s)^{-2}$. Discrimination is even stronger for a Gaussian lineshape, in which case $g_{12}'(\omega_s)$ decreases the same way but $g_{12}''(\omega_s)$ decreases far more rapidly than $(\omega_{12}-\omega_s)^{-2}$. Therefore, by detuning the signal by a few linewidths, the signal loss can be kept almost arbitrarily low without significantly increasing the switching power. A Gaussian lineshape is also highly preferable, as it produces a far lower signal loss. In principle, signal loss is not a concern.

2.2.5 Response Time

After the pump is turned off, electrons in level 2 relax to the ground state (level 1) at a rate commensurate with the total lifetime τ_2. The switch response time is therefore equal to τ_2. Assuming that level 2 relaxes via both a radiative process (time constant $\tau_{rad,2}$) and nonradiative processes (time constant $\tau_{nr,2}$), but that no stimulated processes are present, the total lifetime can be written as:

$$\frac{1}{\tau_2} = \frac{1}{\tau_{rad,2}} + \frac{1}{\tau_{nr,2}} \tag{2}$$

while the radiative lifetime $\tau_{rad,2}$ is given by:[4,22]

$$\tau_{rad,2} = \frac{g_2}{g_1}\frac{m}{e^2 f_{12} K}\frac{\varepsilon_0 c \lambda_{12}^2}{2\pi n} \tag{3}$$

where m and e are the mass and charge of the electron, respectively, f_{12} the oscillator strength of the transition, ε_0 the permittivity of vacuum, and $K=(n^2+2)^2/9$ is the Lorentz correction factor.

In a purely radiative transition, $\tau_2=\tau_{rad,2}$, and the switch response is equal to the radiative lifetime. The parameter that influences $\tau_{rad,2}$ by far the most is the oscillator strength f_{12}, which depends on how strongly allowed the transition is. It varies by as much

as 5 or 6 orders of magnitude for different dopants and transitions, its maximum value being unity for a fully allowed transition. For an IR transition ($\lambda_{12}\approx 1$ μm) with $g_1 \approx g_2$ and a silica-based host ($n\approx 1.46$), the radiative lifetime is smallest for $f_{12}=1$ and equal to ~5 ns. Consequently, for a purely radiative transition, and in the absence of stimulated processes, the switch response time cannot be shorter than a few nanoseconds.

Faster switching can be obtained if a fast nonradiative relaxation process ($\tau_{nr,2} << \tau_{rad,2}$) is present. The response time is then equal to $\tau_2 \approx \tau_{nr,2}$ (see Eq. 2), which can be in the sub-picosecond range.

An important issue is the trade-off between response time and switching power. Equation 1 states that P_{abs}^{π} is proportional to $\tau_{rad,2}/\tau_2$. To minimize the switching power, it is preferable to have a purely radiative transition, in which case $\tau_{rad,2}/\tau_2$ is minimum (and equal to 1). The switching power is then independent f_{12}: a fast and a slow radiative transition require the same power. A high oscillator strength is then preferable, since it minimizes the response time without affecting the switching power.

In contrast, if the transition is strongly nonradiative, the response time τ_2 can be considerably shorter than $\tau_{rad,2}$, as discussed above, but the switching power is greater than the minimum possible value by the ratio $\tau_{rad,2}/\tau_2$. There is therefore a clear trade-off between power and response time. However, the minimum pump pulse energy required for full switching, $E_{abs}^{\pi}=P_{abs}^{\pi}\tau_2$, is independent of the response time: a nonradiative process improves the speed without affecting the switching energy.

2.2.6 Polarization Dependence of Switching Power

In a microscopically and macroscopically isotropic medium, the resonantly-enhanced nonlinear phase shift is independent of pump and signal polarization. In practice, however, the cross sections of an absorber can be anisotropic at the molecular level, even in an amorphous and macroscopically isotropic material such as a glass. The nonlinear phase shift can then exhibit some dependence on polarization. However, this effect is generally quite small. As an example, for the $^4I_{13/2}$-$^4I_{15/2}$ transition of Er-doped silica the relative gain difference for orthogonal signal polarizations is typically under 0.1 dB. The switching power requirement due to this particular transition is thus expected to vary with pump and signal polarizations by at most a few tenths of percent. This conclusion applies to absorbers with moderate anisotropies. This is contrary to the optical Kerr effect, for which a signal polarized parallel to the pump (assumed linearly polarized) experiences a nonlinear phase shift three times larger than a signal polarized perpendicular to the pump.

2.2.7 Summary: Dopant Requirements

Based on the above considerations, to produce an optimum switch (low switching power, high speed, short fiber length requirement), the dopant must exhibit the following ideal properties:

- a transition in the IR (for diode laser pumping and lower switching power))
- purely radiative relaxation (for lower switching power)
- high oscillator strength transition (for shorter response time and shorter device)
- a narrow linewidth (for lower switching power)
- a Gaussian lineshape (for lower signal absorption loss)
- fast nonradiative relaxation (for shorter response time, at the expense of switching power)

2.2.8 Predicted Strength of Resonant Nonlinearities

The above model predicts that with a purely radiative two-level transition in the near IR with a typical linewidth, a phase modulation of π can be produced in the IR in a sub-mm length of high NA fiber with as little as 4 mW of pump power. The corresponding switching power-length product is nearly a billion times smaller than for the intrinsic Kerr effect in the same (but undoped) fiber.

If, in addition, the transition oscillator strength is unity, the switch response time will be a few nanoseconds. Much shorter response times (picosecond or less) are possible if a fast nonradiative process is present, at the expense of a concomitantly higher switching peak power, although the switching energy remains the same, in the 10 pJ range.

The downfalls of the resonantly-enhanced nonlinearity over the Kerr effect are that some of the pump power must be absorbed, and that to benefit from a lower switching power than with the Kerr effect the speed must be limited to the picosecond range.

2.3 Model of Switching with a Multiple-Level Absorber

To model actual dopants more closely, a more general case was developed which investigates a dopant with multiple energy levels, labeled *j*, pumped on the 1->2 transition.

In the absence of pump, only the ground state is populated. The only transitions of the dopant that contribute to the index of the fiber core are the 1->*j* ground state absorptions (GSAs). When a pump is applied, the ground state is depleted and the contributions to the index of *all* GSAs are modified. Also, because the excited state (level 2) becomes populated, all the 2->*j* transitions, which are excited state absorptions (ESAs), are modified and

contribute to the index change. The index change arises from all these transitions, although for most of them the upper level does not get populated.

Modeling shows that in a multiple-level dopant, the nonlinear phase shift is still proportional to the pump power absorbed by the dopant. The contribution of each transition is proportional to the ratio f_{ij}/f_{12} of its oscillator strength f_{ij} to the oscillator strength f_{12} of the 1->2 transition. Of all the contributing transitions, the only ones that produce a significant index change are the few transitions near the signal wavelength (resonant terms), and the transitions with a high oscillator strength f_{ij} (non resonant terms) Most common absorbers exhibit high oscillator strength transitions in the UV. For a signal in the visible or IR, the contributions from UV transitions are independent of signal wavelength.

The effect of UV transitions is larger than that of the 1->2 transition described in Section 2.2 by the ratio f_{ij}/f_{12}. When this ratio is large enough, the switching power is orders of magnitude smaller than with a two-level transition, namely a few to a few tens of microwatts. The downfall again is that a large f_{ij}/f_{12} ratio requires a low f_{12}, i.e. a slow relaxation of electrons from level 2, and thus a slow switch.

2.4 Model of Switching with Semiconductor-Doped Glasses

Semiconductor-doped glasses (SDGs) constitute another type of glasses of interest for nonlinear all-optical switching. We investigated their potential from a theoretical standpoint. Our original motivation was that SDGs exhibit very strong nonlinearities with fast responses. Particular attention was paid to CdSSe- and CdTe-doped glasses, which are commercially available and have been studied experimentally and theoretically by others.

The main physical mechanism responsible for the nonlinearity of SDGs is the same resonantly enhanced nonlinearity studied under this program, except that the absorption properties of a semiconductor are different (parabolic lineshape instead of Gaussian or Lorentzian, and different saturation behavior). Our study involved the development of an original mathematical model of the nonlinearity of SDGs,[14] similar to the model developed for a two-level system in Section 2.2. The objective was to predict the pump power and length requirement of a fiber switch based on this material, and to conduct experimental measurements if the predictions were promising.

The main conclusions of the models are first that the pump and signal wavelengths should be in specific and different ranges to minimize the switching power and signal loss. This is contrary to all experimental work conducted so far on SDGs, which involved self switching (same pump and signal wavelength). Second, this study provided a definitive

calculated value for the nonlinear coefficient of CdSSe-doped glass. It was needed because published values found in the literature span several orders of magnitude. Although the nonlinear coefficient of CdSSe-doped glass predicted by our model is much higher than the nonlinearity of the Kerr effect of silica, it is still relatively small, and much smaller than predicted for other dopants. Third, most of this increase in nonlinearity over the Kerr effect benefits the length requirement, and very little of it goes towards reducing the switching power. As a result, for CdSSe- and CdTe-doped glass the switching peak power is relatively high (2-100 W in a high-confinement fiber) while the required length is short (5-20 mm range). The reason is that the nonlinearity is resonant, as with any absorber but unlike the Kerr effect, so that power can be traded for length over only a limited range.

We provided for the first time an interpretation for the relatively small nonlinearity of these glasses. In a bulk semiconductor, the difference in absorption properties over a standard absorber impacts the nonlinearity model quantitatively but not qualitatively. A bulk semiconductor behaves as an absorber with a high oscillator strength. Thus, based on the two-level model the switching power should be in the 1-10 mW range. This is contrary to both our model prediction and experimental work reported by others. The reason is that when dispersed in a glass matrix to make an SDG, the semiconductor molecules form nanoclusters. In each cluster, surface recombination provides a fast relaxation mechanism from the conduction to the valence band. This mechanism is nonradiative, and much faster (10-20 ps for CdSSe-doped glass) than the radiative lifetime (typically 5-20 ns) of the excited electrons. SDGs therefore have a high $\tau_{rad,2}/\tau_2$ ratio (about 10^3). As in the case of a 2-level absorber (see Eq. 1), this high ratio dramatically increases the peak power requirement of SDGs (by about the same factor of 10^3). On the other hand the response time is much faster (10-20 ps) than the radiative lifetime of the semiconductor. In addition to these limitations, SDGs are known to suffer from photodarkening and low optical damage threshold.

The overall conclusion of this investigation was that in their present form, neither SDGs are competitive for all-optical switching, although because of its longer wavelength bandgap CdTe-doped glass may make a reasonable switch at 850 nm.

All these limitations would be eliminated by designing materials with lower switching powers. To alleviate this problem, we proposed to produce SDGs with larger clusters, which would reduce the rate of nonradiative recombination. This can be accomplished, for example, by annealing the glass after fabrication. This improvement would lead to a material with a slower response time (~1 ns) but a lower switching power (~100 mW) and the same short length requirement (5-20 mm).

2.5 Fiber Switch Architectures

To produce a switch, the doped fiber must be incorporated in an interferometer. The parameters affecting the suitability of an interferometer as a switch include thermal stability, cross-talk, extinction ratio, and the number and internal loss of the components involved (3-dB couplers, WDM couplers, etc.). Cross-talk and extinction ratio are imposed by the performance of individual components, in particular fused fiber couplers. These parameters, as well as the loss of the fiber components, are quite good and suitable for many applications. The number of components is generally small, and not considered to be a significant issue. On the other hand, thermal stability is a key factor which imposes some restrictions on the type and geometry of the interferometers that can be used in practice.

Several stable interferometers have been identified in this study. This section summarizes the findings of this research concerning their suitability, respective pump power and length requirement, and thermal stability.

2.5.1 Mach-Zehnder Interferometer

A good candidate is the Mach-Zehnder (MZ) fiber interferometer, made of two fused fiber couplers spaced by fiber arms. By using WDM couplers, it can be operated so that one optical path is pumped while the other is not, which maximizes the differential phase shift and minimizes the switching power. Also, the phase shift required for full switching is π, which is the lowest requirement of the interferometers retained in this study. Because the two arms are physically separate, however, they must be short, at most a few mm, for good stability with respect to external temperature fluctuations. Such short devices have been demonstrated. Their phase bias, which is set during fabrication, is extremely stable with external changes in temperature.

2.5.2 Nonlinear Directional Coupler

The nonlinear directional coupler (NLDC) is another good candidate. It is a short and thermally stable device. Under this program, we completed a detailed theoretical analysis of the NLDC switching power requirement.[20] So far the NLDC has been used almost exclusively for self switching (the pump switches itself at high enough intensity). The self-switched NLDC requires a power-length product for full switching about 5 times higher than a Mach-Zehnder switch. In this respect the self-switched NLDC is far less advantageous than a MZ switch. To improve this situation, we proposed to use NLDCs for pump-induced switching. We showed that in this mode of operation, if the coupler is

designed optimally, i.e. so that the pump is uncoupled, the power-length product for full switching is only $\sqrt{3}$ times higher than for a MZ switch. This figure is low enough to make the NLDC a good contender for all-optical switching.

2.5.3 Sagnac Interferometer

Another stable switch architecture is the Sagnac interferometer, previously demonstrated successfully utilizing the Kerr effect. In this device, the two optical paths are the two opposite directions of travel along the same fiber (Sagnac loop). An optical circulator placed on each input port of the Sagnac loop can be used to perform the multiplexing/demultiplexing operations needed to separate the pump, the input and the output signals. The recent availability of relatively low loss (<1dB) fiber circulators makes this architecture particularly appealing. The overwhelming benefit of the Sagnac interferometer is that because both signal paths share the same fiber mode, it is largely insensitive to slow external perturbations. Also, the phase shift required for full switching is π, as low as for a MZ switch. This architecture can also be used with resonantly-enhanced nonlinearities provided the loop transit time is several times longer than the nonlinearity response time. It implies that for compactness (a reasonably short loop), the response time must be fairly short, e.g. 1 ns for a 1-2 meter loop.

2.5.4 Two-Mode Fiber Interferometer

All experimental work on resonant nonlinearities carried out under this contract involved dopants with relatively low concentrations. Thus fairly long fibers (~meter) had to be used, precluding the use of a short MS or a NLDC. This is not a fundamental limitation, as many new dopants with extremely large absorption (several dB/mm) are available which will make possible short devices. For practical reasons, this difficulty was overcome by using either a two-mode fiber (TMF) interferometer, or an MZ with long fiber arms.

The TMF is simply made of a fiber that carries two signal modes (LP_{01} and LP_{11}) but (ideally) only the LP_{01} pump mode.[1-3] The signal laser beam is launched into the fiber with a slight lateral offset with respect to the fiber core to excite equal powers in the LP_{01} and LP_{11} modes. At the fiber output, interference between these two modes produces a two-lobe intensity distribution. This distribution depends on the differential phase shift $\Delta\phi$ between the two modes at the output of the fiber. When $\Delta\phi=2m\pi$ (m=integer), the power adds constructively in the vicinity of one of the two lobes of the LP_{11} mode, and destructively in the vicinity of the other lobe: essentially all the power is confined to one lobe. This distribution is reversed when $\Delta\phi$ is incremented by π. For intermediate values of

$\Delta\phi$, the power distribution between the lobes is intermediate and depends on $\Delta\phi$. When a pump is launched into the fiber, the spatial overlap of the LP_{01} pump mode with the LP_{01} signal mode is greater than with the LP_{11} signal mode. Thus, the LP_{01} signal mode undergoes a larger phase shift than the LP_{11} mode, and the output distribution changes. When the pump power is such that the differential phase shift between the two modes is π, the signal power is switched from one lobe to the other. Using this device, the pump-induced phase shift can be inferred by measuring the change in the relative power in one of the two lobes.

The advantage of this architecture is that the two modes utilize the same guiding region and therefore react similarly to environmental changes. We calculated that compared to a MZ, a TMF interferometer is far less susceptible (by a factor of over 1,000) to external temperature fluctuations and steady-state pump-induced heating effects (discussed below). In the laboratory, during actual measurements negligible drift in the TMF output distribution was observed over several minutes. The penalty for this improved stability is that the switching power is larger than in an equivalent MZ switch. The first reason is that both signal modes experience a nonlinear phase shift, and it is the difference between these phase shifts that must amount to π for full switching. Second, a TMF offers a lower optical confinement than a single mode fiber, and the switching power is higher than in a MZ. The first effect increases the switching power by a factor of ~2 to ~4, and the second effect by a factor of up to ~10. Consequently, the switching power measured in a TMF is larger than it would be in an optimized MZ switch by a factor of ~2 to ~40.

In spite of this disadvantage, the TMF is a stable interferometer, easy to implement in the laboratory. It was used extensively in this work as a laboratory test bed to evaluate the nonlinearity of many dopants, as reported in Section 2.6.

Given the superior thermal stability of the TMF, we also investigated its potential as a practical switch. To this end, it is key to be able to butt couple each of the two output lobes of the TMF output into a separate single mode fiber. Similarly, its input must be butt coupled to two single mode fibers to inject the signal and the pump. The TMF will thus become a four-port device. This raises two issues. The first one is how to practically join two fibers to a third fiber? The second issue is how low can the loss of such a junction be, and how high its extinction ratio (ER)? As part of this research, we conducted a detailed theoretical analysis of the second issue. The limitations in both loss and ER arise first from the fact that the two output lobes of a TMF are not symmetric with respect to the axis of the fiber, i.e. the zero intensity point between them is not on axis. Second, the lobes are not circularly symmetric. Finally, even when the two modes of the TMF are exactly in or out of

phase, the weaker lobe always carries a small but non-zero residual power. Our study showed that these problems can be greatly reduced by using an elliptical core TMF.[19] In this case, after optimization of the fiber parameters, a junction between a TMF and two single mode fibers will exhibit a minimum loss of only ~0.25 dB for an ER of 14 dB. By adjusting the position of the single mode fibers slightly differently, the ER can be made infinite at the cost of a slightly higher loss (0.47 dB).[19] These figures suggest that although the loss is a little high, the TMF can potentially be used as a practical switch, provided a viable means of accomplishing the butt junction is devised.

2.5.5 Thermal Stability Considerations

Because in a device based on resonantly enhanced nonlinearity some of the pump power is necessarily absorbed, pump-induced thermal effects are expected. Under the best possible scenario, the pumping and relaxation of electrons from level 1 to level 2 involve no nonradiative processes, all the pump power absorbed by the dopant is ultimately transformed into fluorescence, and there are no pump-induced thermal effects. Under the worst possible scenario, all relaxation processes are dominantly nonradiative, all the absorbed pump power is transformed into heat, and pump-induced thermal effects are maximum. Under the first scenario the power turned into heat is $P_h=0$. Under the second one it is $P_h=P_{abs}^{\pi}$. In general it takes some intermediate value $P_h=\eta P_{abs}^{\pi}$, with $0<\eta<1$.

Assuming some heating is taking place ($P_h\neq0$), two types of effects are present. The first one is the instantaneous effect of a single switching pump pulse, which heats up one of the optical paths more than the other and thus creates a differential thermal phase shift. The second effect is the steady-state thermal phase shift due to the accumulated heating produced by many pump pulses after prolonged operation of the switch. Both thermal effects cause an undesirable change in the interferometer bias. In a nonlinear Sagnac interferometer, the two counter-propagating signals use the same mode in the same fiber almost simultaneously. For any reasonable loop length (under a few hundred meters), both thermal phase shifts are negligible. In the other interferometers considered here, both thermal phase shifts are present, albeit at very low levels in some cases.

We have studied theoretically the instantaneous thermal effect in both a MZ and a TMF. In a TMF, it is over 1000 times weaker than in a MZ, as stated earlier. To study the MZ, we assumed that the pump pulse is short enough that heat dissipation into the cladding during the pulse is negligible. This implies a pulse width τ_p shorter than the heat diffusion time constant τ_{th} of the fiber core. The latter is, for example, ~25 μs for a 5 μm diameter core. For the bias change due to instantaneous heating not to exceed a given value, say -20

dB, the heat released in the core by the pulse must not exceed a certain value, which imposes an upper limit, P_{max}, on the switching power. We showed that for silica, and for a bias change of -20 dB:

$$P_{\max} = 1.67\,10^{10}\,\frac{a^2\lambda_s}{\tau_p \eta} \tag{4}$$

where a is the core radius. The worst possible case (lowest $P_{\max}$) occurs when τ_p is maximum, i.e equal to τ_{th}. Using the expression of τ_{th}, this is $P_{\max}=4.29\ 10^3\lambda_s/\eta$ (in MKSA), or 4.3 mW for $\lambda_s=1$ μm and $\eta=1$ (100% of the absorbed pump turned into heat). This is comparable to the lowest possible $P_{abs}{}^{\pi}$ for a 2-level dopant. Consequently, the phase shift due to instantaneous heating can exceed the nonlinear phase shift. On the other hand, with $\eta \leq 0.1$ and a short enough pulse ($\tau_p \leq 0.5$ μs), $P_{\max} \geq 330$ mW, which is much larger than the $P_{abs}{}^{\pi}$ of a good dopant, and the instantaneous thermal effect is minimal.

The general conclusions are that first, instantaneous thermal effects vanish for a dopant with a two-level pumping scheme and a purely radiative transition (in which case $\eta=0$). Second, for a good dopant, and even if $\eta=1$, instantaneous thermal effects are negligible if the pump pulse is shorter than ~100 ns. Meeting this last condition imposes a high oscillator strength transition (to allow short pump pulses).

Steady-state thermal effects were also modeled. It was found that this effect can be greatly suppressed by providing a path for rapid heat exchange between the two fibers or waveguides, thus minimizing their steady-state temperature difference. Such a path already exists in NLDCs, since the two waveguides are very close to each other. In a fiber MZ the same can be accomplished by establishing good thermal contact between the fiber arms, with a grease or by partially fusing them together. Steady-state thermal effects are therefore not as critical as instantaneous heating.

2.6 Experimental Fiber Switches

Under this program, several dopants were tested in TMF and MZ interferometers, (1) to demonstrate the predicted strength of resonantly enhanced nonlinearities, (2) to verify the predicted relationships between power, length and speed, (3) to identify and test dopants with high oscillator strength transitions, and (4) to identify and test potential dopants that would ultimately lead to practical switches. This section summarizes the results of this experimental work.

2.6.1 Er-Doped Fibers

Trivalent rare earth ions were the first dopants to be tested.[1-5,7,10-13,15,17,18,21,22] They constituted an excellent test bed because they possess numerous visible and IR transitions (convenient for pumping with diode lasers), are routinely incorporated in silica-based fibers, easily available, and their spectroscopy is well-understood. Their main disadvantage is that these transitions take place between energy levels of same parity. Consequently, the metastable levels of trivalent rare earths exhibit long radiative lifetimes (>100 ns), or equivalently low oscillator strengths. Also, rare earth concentrations in silica are generally low, which means long fibers need to be used.

Pump-induced index changes were first studied in an Er-doped fiber.[1,3,4] Very low switching powers were reported. In a 95-cm long TMF pumped with a 1.48 μm diode laser, full switching at 920 nm was observed with $P_{abs}{}^{\pi}$=8 mW only (see Table 1). This value corresponds to a nonlinear coefficient about 140,000 times stronger than the intrinsic Kerr effect of silica. The dopant-induced signal loss was only 0.25 dB. If the TMF was replaced with a MZ made with a high NA fiber, the switching power would be reduced to 1.4 mW, which is comparable to what has been observed by other authors.

Dopant	λ_S (nm)	λ_p (nm)	Length (m)	$P_{abs}{}^{\pi}$	τ_2	$E_{abs}{}^{\pi}$ (μJ)	Ref.
Er^{3+}	920	1480	0.95	8 mW	8 ms	64	1,4,13,21
Nd^{3+}	633	807	1.0	5 mW	380 μs	1.9	3,2,13
Nd^{3+}clusters	633	807	1.0	2.5 W	400 ns	1.0	2,13
POHC	900	532	0.22	6W	<25 ns	0.15	8,16,13
V^{3+}-V^{4+}	1320	1064	1.0	50 mW	3.5 μs	0.18	17,13

Table 1. Measured characteristics of this program's doped fiber switches.

The signal wavelength (920 nm) was originally selected for its proximity to the $^4I_{15/2}$->$^4I_{11/2}$ transition of Er^{3+}, which was expected to produce a strong resonant contribution. To verify this point, the nonlinear phase shift was measured at constant pump power (P_{abs}=10 mW) for a range of signal wavelengths (Fig. 2).[15,17,21,22] The experimental data points distinctly showed the presence of several resonances, due to known GSA and ESA transitions in Er^{3+}, superimposed on a large, weakly wavelength dependent contribution originating from the strong VUV transitions of Er^{3+}. The solid curve in Fig. 2

is a fit of our theoretical model to the data. It was plotted using the six GSAs and three ESAs of Er^{3+} that affect the spectral range of Fig. 2, and the first group of five GSA and five ESA transitions in the VUV. For the latter, the oscillator strengths were assumed identical and used as a single fitting parameter. The fitted value which gave the solid curve of Fig. 2 is f_{UV}=0.004, which is close to the value calculated independently from VUV absorption spectra. The fit is reasonably good. The contribution of the VUV transitions alone is shown in Fig. 2 as the dashed curve. Since this earlier work, we have shown experimentally that dominant VUV contributions are present in other dopants, in particular Nd^{3+} and Yb^{3+}.[17]

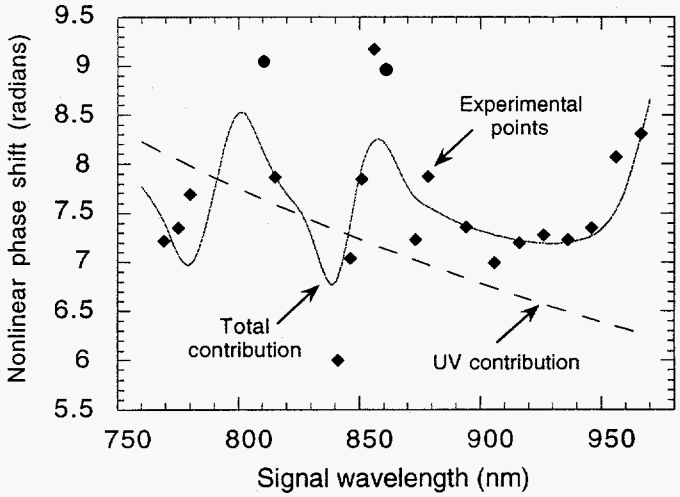

Fig. 2. Measured and calculated phase shift vs signal wavelength in an Er-doped fiber pumped with P_{abs}=10 mW from a 1480-nm diode laser.

This result confirmed for the first time that (1) the strong nonlinearity observed in Er-doped fiber originates mostly from VUV transitions, (2) in the IR the nonlinearity depends weakly on wavelength, and (3) operation in the IR is broadband.

Since this work, switching with a considerably lower switching power (~50 μW) and shorter fiber (3 cm) was reported in an Er-doped fiber grating, although this value was partly due to thermal effect and resulted in a low extinction ratio (10 dB).

At this point the two issues that needed to be addressed for practical devices were reducing the response time and the fiber length. As discussed earlier, the former is imposed by the relaxation time of the metastable lifetime of Er^{3+}, about 10 ms for Er^{3+}. To increase the switching speed, one option was to select a dopant with a shorter lifetime, such as Nd^{3+} ($\tau_{rad,2}$~400 μs).

2.6.3 Fibers Doped with Color Centers

Because of their low pump absorption (at best tens of dB/m) and low concentrations, trivalent rare earths are not likely to produce short devices. To reduce the length and increase the speed, one must utilize dopants with a higher oscillator strength transition and/or higher concentrations. Color centers are good candidates. They can have transitions in the IR with a high oscillator strength, and high concentrations are possible in silica. However, they often suffer from photostability problems, which rules out a large number of potential color centers.

We demonstrated the usefulness of this class of dopants with phosphorus-oxygen hole centers (POHC), known to possess absorption transitions in the visible range with oscillator strengths near unity. Also, high concentrations of POHC can easily be created in readily available phosphorus-doped fibers by γ-ray irradiation. Another advantage is that the nonlinear region can be created selectively only where it is needed by irradiating the targeted region, thus avoiding pump absorption in undesirable areas (like in the fiber pigtails). The experimental switch used a 22-cm length of P-doped fiber that was irradiated with 100 krad of 0.68 MeV γ-rays.[8,16] The fiber was pumped with 532-nm, 200-ns pulses and the nonlinearity was measured at 900 nm in a TMF. The switching peak power was $P_{abs}{}^{\pi} \approx 6$ W, and the response time was well under 25 ns (~1 ns predicted by theory) (see Table 1).[8,16] With an optimized fiber (high-confinement, high γ-ray dose), one could make a 1.064-μm fiber MZ switch a few mm long with $E_{abs}{}^{\pi}$ of only 0.6 nJ. Unfortunately, POHCs were observed to photobleach at the pump wavelength and intensity used, resulting in nearly complete loss of absorption after a few hours of operation. In spite of this shortcoming, this experiment confirmed that switching is possible in a short length of fiber, with a nanosecond response time, and with the same nominal switching energy as a slow switch.

2.6.4 Fibers Doped with Transition Metal Ions

The interest in this group of dopants arises from the fact that transition metals exhibit near-IR absorptions with sizable oscillator strengths, typically around 10^{-2}. They are also easy to incorporate in the core of a silica-based fiber in fairly high concentrations (several wt. %).[13] The potential of this class of dopants was tested in a fiber doped with vanadium.[17] The fiber absorption spectrum showed a broad absorption from about 600 to 1100 nm, which suggests that the metal was in several degrees of oxidations, although

2.6.2 Nd-Doped Fibers

The first demonstration of a Nd-doped fiber switch utilized a TMF and a signal at 632.8 nm, selected for its proximity to the strong $^4I_{9/2}$->$^4G_{5/2}$ GSA of Nd^{3+} (~590 nm).[2,3] The TMF was an elliptical core fiber with an advantageously high optical confinement. The pump source was a Ti:sapphire laser (at ~820 nm). When the fiber was pumped continuously, we measured $P_{abs}{}^{\pi}$=5 mW for a length of ~1 m (see Table 1). Full switching was also observed in a much shorter fiber (8.2 cm) with heavier doping (1 wt.% Nd_2O_3), although it was pumped at 514.5 nm and its $P_{abs}{}^{\pi}$ was thus higher (~60 mW) because of pump ESA.[3]

To investigate the switch dynamic response, the pump was chopped into 2 ms pulses at 250 Hz, and the power in the switched lobe recorded versus time.[2] The relaxation of the switch showed a fast component (~μs) followed by a slow component equal to the radiative lifetime of Nd^{3+} (~380 μs). This behavior was attributed to the presence of clusters in the fiber,[2,3] due to the fiber's high Nd concentration and the absence of network modifiers in the glass. We studied this problem in detail.[6,11] A fast nonradiative energy transfer occurs between ions of a cluster, not present when ions are isolated, which accounts for the presence of a fast component. Our studies generated for the first time general rate equations for clusters comprising multiple ions,[10] which lead to a new experimental method to identify the mean size of clusters.[11] The model predictions were also consistent with the observed dynamic behavior of the Nd-doped fiber switch.

This fast relaxation mechanism was used to produce sub-microsecond switches in clustered Nd-doped fiber.[2] The switch was pumped with Q-switched ~125 ns FWHM pulses from the same pump laser at a high repetition rate (600 kHz). The switching power was then 2.5 W (see Table 1). This value is higher than under cw pumping because the same energy was delivered to produce the required population change but in a much shorter time. Because the pulse repetition rate is much higher than $1/\tau_{rad,2}$, the slow component did not contribute to any measurable decay in the switched power between consecutive pump pulses.[7] Instead, the output of the switch was a series of switches signal matching the sequence of pump pulses. The decay time of the switch was measured to be ~380 ns. Since $P_{abs}{}^{\pi}$ is proportional to $\tau_{rad,2}/\tau_2$ (see Eq. 1), the penalty for this improved speed is a commensurate increase in switching peak power, as observed (2.5 W versus 7.5 mW, consistent with $\tau_{rad,2}/\tau_2 \approx 10^3$).

mostly V^{3+} and V^{4+}. The test bed was a fiber MZ containing a 1-m length of V-doped fiber operated at 1.32 μm, where absorption loss due to vanadium is low. Under cw pumping, the switching power was measured to be $P_{abs}{}^{\pi}$≈50 mW when it was pumped at 1064 nm, and 100 mW with a pump around 800 nm.[17] The response time was 3.5±1.5 μs (see Table 1).

This result can be improved significantly in a straightforward manner. First, the vanadium concentration in this trial fiber was very weak, estimated at ~16 wt. ppm V. Since higher concentrations can be produced, the same performance can be expected in a cm-long, more highly doped fiber. Second, by improving the optical confinement, $P_{abs}{}^{\pi}$ would be reduced to only 14 mW. Finally, although this point is speculative, based on the measured lifetime of V-doped YAG it is possible that ions in the right degree of oxidation may lead to response times as short as 10 ns with no switching power penalty. Even without this last improvement, in its present state this dopant combines a moderate switching speed and a low switching power. It is an excellent candidate for a laser-diode pumped microsecond switch.

3. Conclusions

Both theoretical and experimental investigations have established that resonantly-enhanced nonlinearities introduced by an absorber in silica fibers or waveguides are very promising. Modeling predicts that the effect can be up to nearly 10^9 times stronger than the only other contender for all-optical switching in silica fibers, namely the Kerr effect. This is strong enough to switch IR signals with very low pump powers, in extremely short fibers, with virtually zero signal loss and response times in the nanosecond range. Much faster response times are also possible, and have been demonstrated, at the cost of higher switching powers.

Switches evaluated so far in the laboratory have demonstrated this potential with several dopants. With rare earths, full switching requires only as little as 1 mW in a meter-long Mach-Zehnder fiber interferometer. The best devices had a power-length requirement for full switching more than 10^5 times lower than with the Kerr effect. The presence of strong UV transitions contributes strongly to this nonlinearity, in rare earths and probably of other dopants as well. The response times of rare earths are unfortunately fairly long (>100 μs). Other dopants have lead to much shorter response times, for example vanadium, which required as little as 15 mW for a response time of a few μs. Responses in the ns to tens of ns range are also possible (for example under 25 ns for 2.5 W of peak power in phosphorus oxygen hole color centers). In all cases, full switching requires a pump energy

in the range of only 0.1 to a few nJ, independently of the speed. Importantly, these nonlinearities remain strong and are weakly wavelength dependent for signals in the IR, so that they are extremely well suited for operation at 1.3 and 1.55 μm.

The characteristics of these switches demonstrate the tremendous potential of resonantly-enhanced nonlinearities: short all-fiber switches (<1 cm) with negligible internal loss (<0.1 dB), low switching power (<10 mW), short response time (~1-10 ns), IR pump sources and operation throughout the IR. Much faster response times are possible without changing the switching energy by utilizing nonradiative relaxation processes.

In order to fully benefit from the potential of this nonlinearity, one must still identify dopants possessing a high oscillator strength transition and a reasonable solubility in silica-based glasses. While waiting for such advances to be made, some dopants have already been identified which can readily yield practical IR switches. A particular candidate is vanadium, which can produce a switch with a μs response time made of a short fiber MZ (~1 cm) pumped with only ~15 mW from a laser diode.

4. Publications

1. R. H. Pantell, R. W. Sadowski, M. J. F. Digonnet, and H. J. Shaw, "Laser-Diode-Pumped Nonlinear Switch in Erbium-Doped Fiber," *Opt. Lett.* **17**, 1026-1028 (July 1992).

2. R. W. Sadowski, M. J. F. Digonnet, R. H. Pantell, and H. J. Shaw, "Microsecond Optical-Optical Switching in a Neodymium-Doped Two-Mode Fiber," *Opt. Lett.* **18**, 927-929 (June 1993).

3. R. W. Sadowski, M. J. F. Digonnet, R. H. Pantell, and H. J. Shaw, "Resonantly-Enhanced Nonlinear Optical Switching in Rare Earth Doped Fibers," in *SPIE Proceedings on Fiber Laser Sources and Amplifiers*, vol. 1789, (SPIE, Washington, 1993), pp. 98-111.

4. R. H. Pantell, M. J. F. Digonnet, R. W. Sadowski, and H. J. Shaw, "Analysis of Nonlinear Optical Switching in an Erbium-Doped Fiber " *J. Lightwave Technol.* **11**, 1416-1424 (September 1993).

5. R. H. Pantell, and M. J. F. Digonnet, "A Model of Nonlinear All-Optical Switching in Doped Fibers," *J. Lightwave Technol.* **12**, 149-156 (January 1994).

6. M. K. Davis, M. J. F. Digonnet, R. H. Pantell and H. J. Shaw, "Novel Techniques to Characterize Clustering in Doped Fibers," in *SPIE Proceedings on Fiber Laser Sources and Amplifiers V*, vol. 2073 (SPIE, Washington, 1994), pp. 50-64 [Invited Paper].

7. R. W. Sadowski, M. J. F. Digonnet, R. H. Pantell, and H. J. Shaw, "Sub-Microsecond All-Optical Switching in Nd-Doped Fibers," in *SPIE Proceedings on*

Fiber Laser Sources and Amplifiers V, vol. 2073 (SPIE, Washington, 1994), pp. 166-171.

8. R. W. Sadowski, M. J. F. Digonnet, R. H. Pantell, and H. J. Shaw, "All-Optical Switching using Color Centers in Irradiated Silica Fibers," in *SPIE Proceedings on Doped Fiber Devices and Systems*, vol. 2289 (SPIE, Washington, 1994), pp. 110-116.

9. D. Mayweather, M. J. F. Digonnet, R. H. Pantell, and H. J. Shaw, "Power and Length Requirements for All-Optical Switching in Semiconductor-Doped Glass Waveguides," in *SPIE Proceedings on Doped Fiber Devices and Systems*, vol. 2289 (SPIE, Washington, 1994), pp. 125-133.

10. M. J. F. Digonnet, M. K. Davis, and R. H. Pantell, "Rate Equations for Clusters in Rare-Earth Doped Fibers," *J. Opt. Fiber Technol.* **1**, 48-58 (October 1994).

11. M. K. Davis, M. J. F. Digonnet, and R. H. Pantell, "Characterization of Clusters in Rare Earth-Doped Fibers by Transmission Measurements," *J. Lightwave Technol.* **13**, 120-126 (February 1995).

12. M. J. F. Digonnet, R. H. Pantell, H. J. Shaw, J. R. Simpson, and M. Yan, "Advances toward Practical All-Optical Fiber Switches," in *Optical Fiber Communication - Technical Digest Series,* vol. 8 (Optical Society of America, Washington, D.C., 1995), pp. 15-16.

13. R. W. Sadowski, in *Nonlinear All-Optical Switching in Doped Silica Fibers*, PhD Thesis, Electrical Engineering Department, Stanford University, CA, June 1995.

14. D. Mayweather, M. J. F. Digonnet, and R. H. Pantell, "Parametric Analysis of Semiconductor-Doped Glasses for All-Optical Switching," *J. Lightwave Technol.* **14**, 601-610 (April 1996).

15. R. W. Sadowski, M. J. F. Digonnet, H. J. Shaw, and R. H. Pantell, "Proposed Role of Strong UV Transitions in the Enhanced Nonlinearity of Doped Fibers," *Materials Research Society Conference*, San Francisco, California (April 1996).

16. R. W. Sadowski, M. J. F. Digonnet, R. H. Pantell, H. J. Shaw, Jay R. Simpson, and Man Yan, "All-Optical Switching using Color Centers in an Irradiated Phosphorus-Doped Fiber," *IEEE Photon. Technol. Lett.* **8**, 897-899 (July 1996).

17. M. J. F. Digonnet, R. W. Sadowski, H. J. Shaw, and R. H. Pantell, "Contribution of UV Transitions to the Strong Third Order Nonlinearity of Doped Fibers," to be published in *SPIE Proceedings on Doped Fiber Devices* (SPIE, Washington, 1996).

18. R. W. Sadowski, M. J. F. Digonnet, H. J. Shaw, and R. H. Pantell, "Low power, microsecond all-optical switching in vanadium doped fiber," to be published in *SPIE Proceedings on Doped Fiber Devices* (SPIE, Washington, 1996).

19. M. Arbore, M. J. F. Digonnet, and R. H. Pantell, "Analysis of the Insertion Loss and Extinction Ratio of Two-Mode Fiber Interferometric Devices," to appear in *J. Lightwave Technol.*

20. M. K. Davis and M. J. F. Digonnet, "Switching Power Reduction using a Pumped Nonlinear Directional Coupler," to appear in *Photon. Technol. Lett.*

21. M. J. F. Digonnet, R. W. Sadowski, H. J. Shaw, and R. H. Pantell, "Experimental Evidence for Strong UV Transition Contribution in the Resonant Nonlinearity of Doped Fibers," to appear in *J. of Lightwave Technol.*

22. M. J. F. Digonnet, R. W. Sadowski, H. J. Shaw, and R. H. Pantell, "Resonantly-Enhanced Nonlinearity in Doped Fibers for Low-Power All-Optical Switching: A Review," to appear in *J. Opt. Fiber Technol.*, (January 1997).[Invited].

23. R. W. Sadowski, M. J. F. Digonnet, R. H. Pantell, H. J. Shaw, "A Vanadium-Doped Fiber All-Optical Switch." to be submitted to *Opt. Lett.*

5. Patents (Issued and Pending)

1. *Nonlinear Optical Coupler Using a Doped Optical Waveguide*, R. H. Pantell, R. Sadowski, M. J. F. Digonnet, and H. J. Shaw, S92-025, STANF.99A, Patent Number: 5,311,525 (May 1994).

2. *Laser-diode-pumped Nonlinear Switch in Erbum-doped Fiber*, R. H. Pantell, R. Sadowski, M. J. F. Digonnet, and H. J. Shaw, S92-025, STANF.99A (June 1991).

3. *Enhanced Third Order Nonlinearity in Optical Waveguides and Miniature Low Power Nonlinear Devices*, R. H. Pantell and M. J. F. Digonnet, S91-091 (August 1991).

4. *Stable Nonlinear Mach-Zehnder Fiber Switch*, M. J. F. Digonnet, H. J. Shaw, S. Lacroix, R. Pantell, and R. Sadowski, S95-042 (May 1994).

DISCLAIMER

This report was prepared as an account of work sponsored by an agency of the United States Government. Neither the United States Government nor any agency thereof, nor any of their employees, makes any warranty, express or implied, or assumes any legal liability or responsibility for the accuracy, completeness, or usefulness of any information, apparatus, product, or process disclosed, or represents that its use would not infringe privately owned rights. Reference herein to any specific commercial product, process, or service by trade name, trademark, manufacturer, or otherwise does not necessarily constitute or imply its endorsement, recommendation, or favoring by the United States Government or any agency thereof. The views and opinions of authors expressed herein do not necessarily state or reflect those of the United States Government or any agency thereof.